Steel and Composite Structures, Vol. 7, No. 1 (2007) 1-18
DOI: http://dx.doi.org/10.12989/scs.2007.7.1.001

Improvements to the analysis of floorbeams with additional web cutouts for orthotropic plated decks with closed continuous ribs

Wouter De Corte† and Philippe Van Bogaert‡

Department of Civil Engineering, Ghent University, Ghent, Belgium

(Received December 1, 2005, Accepted July 14, 2006)

Abstract. Additional cutouts in the floorbeam webs of orthotropic plated bridge decks relieve the highly stressed lower flange of the ribs passing through these floorbeam webs from possible fatigue damage. Conversely, the floorbeam webs themselves suffer from high stress concentrations, especially along the free edges of the additional cutouts. These stresses result from a combination of direct introduction of vertical traffic loads in the weakened web and from the truss action of the floorbeam. The latter differs from a simple beam action due to the presence of the openings and corresponds more to the behaviour of a Vierendeel truss. Close assessment of the appearing stresses, highly relevant for fatigue resistance, requires the use of elaborate finite element modelling. However, a full finite element analysis merely provides the results of total stresses, leaving the researcher or designer the difficult task of finding the origin of these stress components. This paper presents a calculation method for cutout stresses based on a combination of a framework analysis and a two dimensional finite element analysis of much smaller parts of the floorbeam. This method provides more insight in the origin of the stress components, as well as it simplifies any comparison of different additional cutout geometries, independent of the floorbeam topology.

Keywords: orthotropic plated deck; floorbeams; closed ribs; web cutouts; stress concentrations.

1. Introduction

The behaviour of floorbeams in orthotropic plated decks with closed continuous ribs is substantially different from that of an average beam, especially if additional cutouts are used around the bottom flange of the longitudinal ribs. As a first consequence, it appears that the vertical deformations are much larger than expected, thus influencing the load transfer from directly loaded to non loaded ribs (Pelikan and Esslinger 1957, Wolchuk 1963, Troitsky 1968, and De Corte and Van Bogaert 2006). A second consequence concerns the calculation of the stresses in the floorbeam web itself. When comparing measured or FE calculated stresses with results from classical beam theory it becomes clear that the stress distribution in the web in no way relates to the one in a simple beam. It relates much more to the distribution found in a special truss without diagonal members commonly referred to as a Vierendeel truss. Based on this observation, a calculation model was proposed by Haibach and Pläsil (1983). In his proposal, the floorbeam is simplified to a Vierendeel truss. Traditional framework

†Post doctoral Researcher, Corresponding author, E-mail: Wouter.DeCorte@UGent.be
‡Professor, E-mail: Philippe.VanBogaert@UGent.be

analysis methods can then calculate the internal forces, and from these forces the stresses in the flanges and the web of the real floorbeam are derived.

Noticeably, Haibach points out that the calculation method is incomplete since it does not clarify the high stress concentrations around the cutout edges calculated and measured by various authors (Beales 1990, Wolchuk 1992, Dexter and Fisher 1995, Van Bogaert and De Corte 2001, and De Corte and Van Bogaert 2002). Evidently, a framework analysis can produce only triangular stress patterns across the width of each member. The combination method presented in this paper acknowledges the Vierendeel analogy, in addition to providing reliable results for the edge stresses as well. This is done by a combination of the Vierendeel truss analogy with the result of a finite element calculation based on reduced models of the floorbeam web, containing the cutout geometry. This configuration allows comparing various types of cutout geometries independent from the floorbeam characteristics.

Apart from the beam action, a large portion of the stress concentrations relates to the introduction of vertical traffic loads acting directly on the floorbeam. Since openings appear in the web, the loads will attempt to close these, thus creating large compression stresses around the edges. Again Haibach acknowledges this phenomenon but does not provide an adequate calculation method. In a similar way as for the beam stresses, the stress pattern resulting from the introduction of vertical loads can be calculated as a function of the exact cutout geometry. Both types of stresses act independently, and in a linear elastic analysis, as used for fatigue verifications, the stresses resulting from the truss action and the direct load introduction can simply be added.

In a first part of the paper, the Vierendeel model as introduced by Haibach will be discussed. Subsequently, the combination model is presented and illustrated by a numerical example. Finally the validity of the model for other combinations of floorbeam characteristics is demonstrated, and alternative cutout geometries are compared.

2. The framework analogy according to Haibach and Pläsil

The principle of the Vierendeel analogy was first suggested in the publication by Haibach and Pläsil (1983). Based on experimental strain gauge results, the authors propose to model floorbeams according to Fig. 1. In this model, the upper chord is equivalent to the actual deckplate. However, the effective width of the chord needs to be determined taking into account possible shear lag. The chord is then pinned to vertical posts consisting of 2 parts. The upper part has finite axial and flexural stiffnesses. It reflects the web area between the lower point of the cutout and the deckplate. This part is commonly referred to as the "tooth" because of its tooth-like appearance. The stiffness characteristics are determined by considering the width of the undisturbed web at halfway the rib's height. The lower part with infinite stiffness reflects the non disturbed web area between the position of the lower chord of the model and the lower point of the cutout. Finally, the last part of the Vierendeel analogy is the lower chord. This chord consists of the lower flange of the floorbeam and the non disturbed web area forming an inverted T section in the substitute model. Its axis is located at its centre of gravity. Evidently, the distance between the posts is equal to the rib spacing, and in the calculation the contribution of the ribs is neglected.

The internal forces are calculated using traditional analytical methods for framework analysis as implemented in computer software. As by a result, large horizontal shear forces are found in the vertical posts which can be related to bending moments and triangular bending stress distributions at the location of minimal web area (Fig. 2). In addition to these truss action related stresses, the direct load

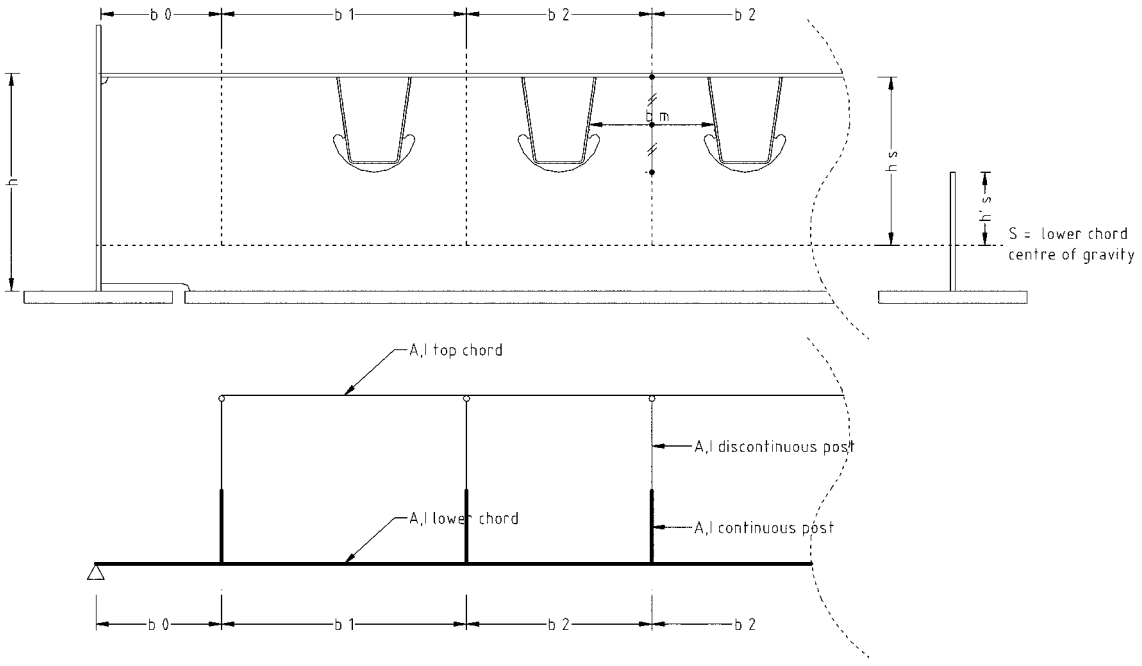

Fig. 1 General outline of the Vierendeel analogy for the calculation of the floorbeam stresses

introduction stresses need attention as well. Haibach proposes a uniform load dispersal over an angle of 35° (Fig. 2) and simple addition of the resulting stresses to the beam related stresses. As pointed out by Haibach, both the triangular stress distribution due to the transverse bending as well as the uniform load dispersal for the direct introduction of vertical loads cannot be correct and require a more detailed model. Clearly the stresses at the cutout edge are related to the shape of the cutout itself as well as to the general floorbeam characteristics, such as length, height, and rib spacing. As will be demonstrated in

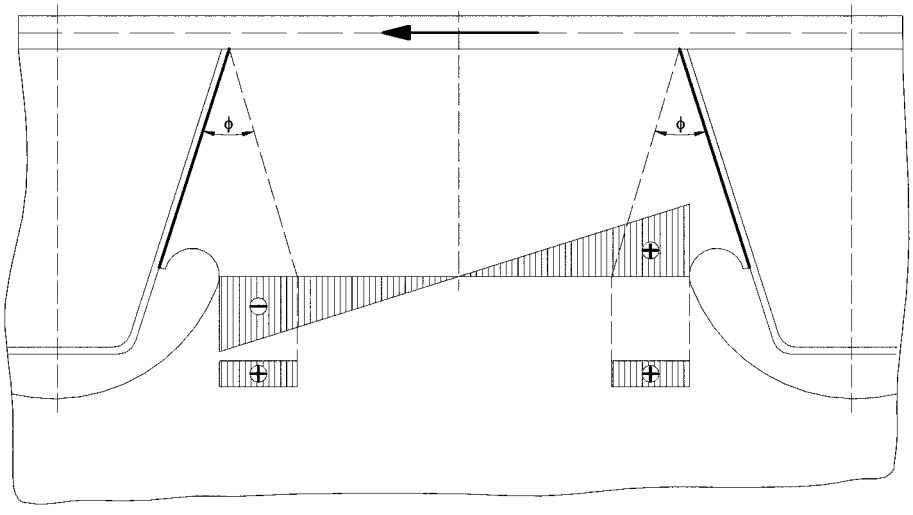

Fig. 2 Stress distribution in the floorbeam web according to Haibach and Pläsil

this paper, the cutout shape has a large influence on the magnitude of the stress concentrations as well as on the location of the peak stress which does not necessarily coincide with the location proposed by Haibach.

The method presented in this paper recognises the Vierendeel model but introduces a shape factor relating the internal forces in the Vierendeel model to the stresses at a critical location along the cutout edge. This shape factor is related only to the actual cutout shape and can therefore be computed in a simpler manner. Furthermore, it enables a fair comparison of cutout shapes independent of the overall floorbeam geometry.

In addition to the requirement for the introduction of a shape factor, a modification to the calculation of the internal forces in the Vierendeel truss is equally needed. The traditional computation of these forces follows directly from flexural and axial deformation and does not consider shear deformation. For the upper and lower flange, this approximation can be applied with sufficient accuracy. In contrast, this approximation certainly is no longer valid for the calculation of the deformations of the vertical posts. In that case, the share of shear deformation cannot be neglected. Various computation methods can be used to assess the influence of shear deformation. A first possibility is the use of improved framework analysis formulae including shear deformation. However, as shear deformation is rarely important in practice, most of the commercially available software does not offer such inclusion. A second possibility is the adaptation of the posts flexural stiffness to a ficticious value leading to equal deformation for the specific configuration of the vertical posts. Finally, a third possibility is to derive an equivalent stiffness by using finite element models of the cutout geometry, provided the FE-code automatically takes shear deformation into account.

3. The combination model : Vierendeel analogy with shape factor

The extension of the Vierendeel analogy requires the introduction of a shape factor. The principle is illustrated in Fig. 3. The complete floorbeam is simplified according to the principles mentioned in paragraph 1, and the vertical loads are applied to the upper chord. The horizontal shear forces in the vertical posts, resulting from this condition, are labeled condition A shear forces. Subsequently, a small but detailed finite element model is created of a single vertical post, having identical geometry as the web cutout of the actual floorbeam. At the top edge of this post, a uniformly distributed horizontal unity load is applied. This unity load creates a certain stress distribution in this post. Especially interesting are the stress values at the free edge of the cutout. Of these, the maximum value is labeled condition B stress and its location is noted. The condition B stress can be considered a geometric shape factor, as it is specific for that geometry and found under a unity load. Finally, multiplication of the condition A shear forces with the condition B stress results in the maximal stresses due to the girder action left and right of each longitudinal rib. Furthermore, these maxima should be equal to those found from a full finite element analysis. However, the above described method is not valid for the first and the last vertical post due to their asymmetric shape. Nevertheless these are generally wider than the normal posts making the stresses found in these posts less critical.

Evidently the Vierendeel analogy produces only the stresses related to the truss action. The stresses produced by the introduction of vertical traffic loads are computed in a similar way, again by application of the reduced “single tooth” finite element model. On this element and in multiple load cases, vertical concentrated loads are applied in a number of points of the top edge resulting in an influence line for load introduction at the location of maximum stress. Integration of this influence line

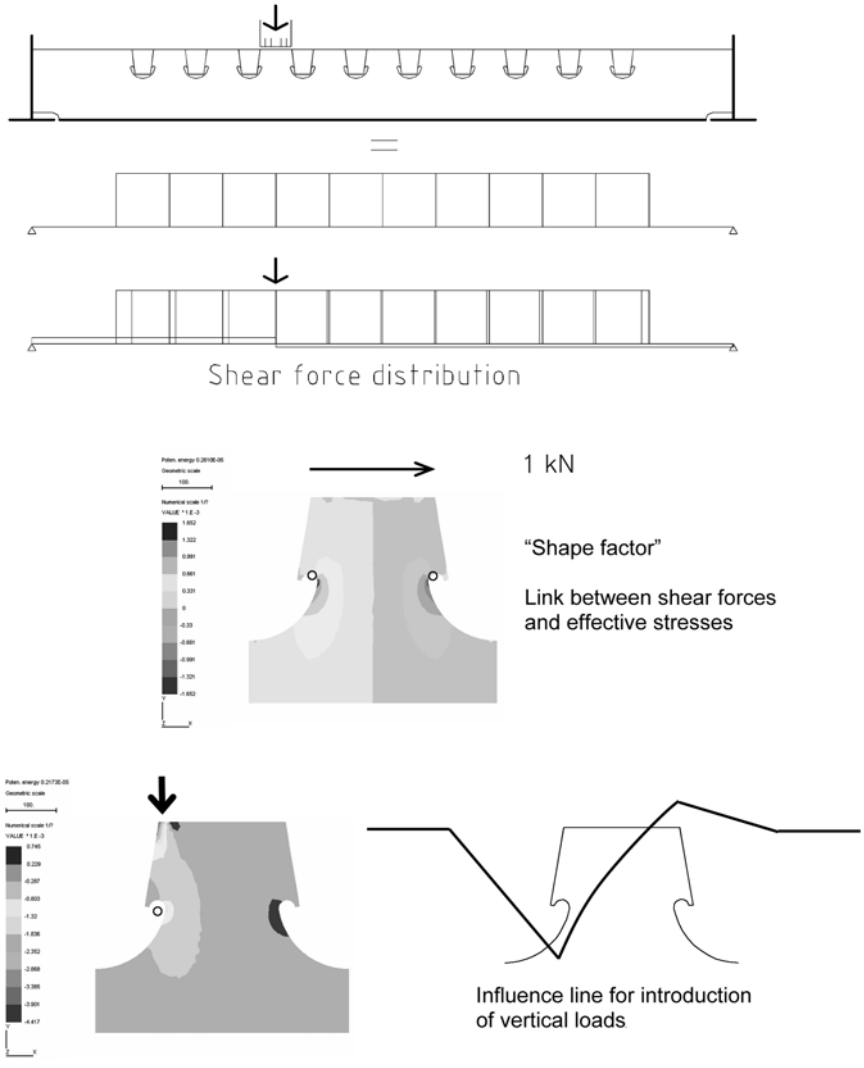

Fig. 3 Principle of the combination model : Vierendeel analogy with shape factor

across the width of the load gives the effective maximum stresses at the critical locations due to transfer of the vertical loads. Both actions are assumed to act independently, and linear elastic stresses from both origins in corresponding locations can simply be added.

4. Illustration of the combination model

A numerical example illustrates the use of the combination model, and a parametric study will demonstrate the applicability of the combination model for other dimensions. The example is based on the dimensions of Table 1. With this example, the assumption that truss action and introduction of vertical loads are independent actions will be proven by comparison of full finite element results to

Table 1 General orthotropic deck dimensions as used throughout the paper

Floorbeam span	10000 mm
Number of ribs	10
Floorbeam web dimensions	1000 mm × 20 mm
Deckplate dimensions	4000 mm × 15 mm
Floobeam bottom flange dimensions	600 mm × 40 mm
Rib height	350 mm
Rib width (U = upper / L = lower)	300 (U) - 200 (L)
Rib wall thickness	8 mm
Rib spacing	750 mm
Additional cutout shape	Haibach type

results found from the combination model. For this, two situations are considered. A first situation concerns the floorbeam completely supported across its entire length. This configuration excludes any truss action. In this way, stresses resulting from the introduction of vertical traffic loads are isolated from truss action related stresses. The second situation is found by subtracting the results of situation 1 from the results of the actual configuration, with actual support conditions. This second situation renders stresses due to truss action only. In this manner the two actions are practically separated. After proof for this separation is established, the results from both actions can be compared independently with the results of the combination model.

4.1 Structure of the web post

The relatively simple two dimensional finite element model of a single tooth represents one vertical post between two adjacent ribs (Fig. 4). The lower and side edges of the web post, as cut from the floorbeam web, are fully restrained. All remaining edges can deflect freely, except the top chord for the case of the load introduction. In the latter case the – non modelled – deckplate areas left and right of the area under consideration are re-introduced and modelled as hinged rods. They are connected to fixed points corresponding to the opposite boundaries of the web openings. These conditions correspond to

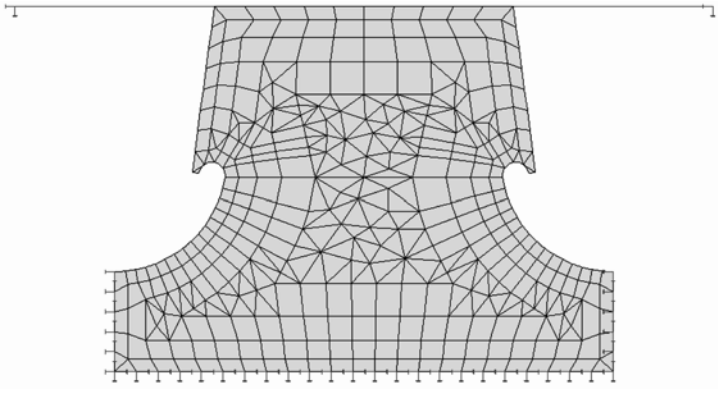

Fig. 4 Two dimensional finite element model of a single tooth

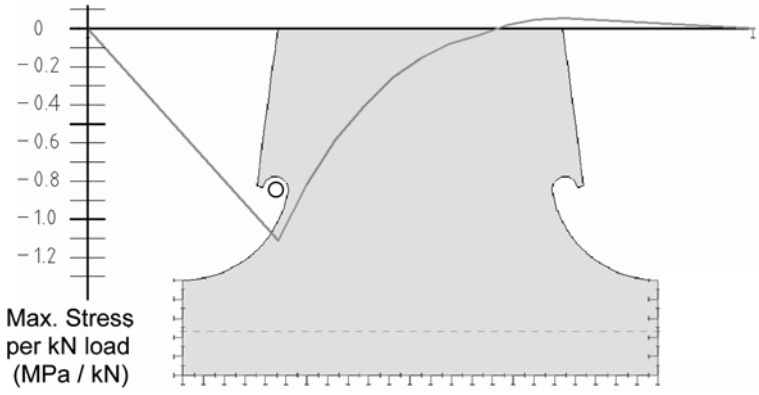

Fig. 5 Influence line for maximum edge stresses as a result of the introduction of vertical traffic loads

the actual situation where the deformation of the deckplate is constrained by adjacent non loaded web areas. Evidently, for the truss related stress, these constraints do not need an entry in the web post model since they are explicitly present in the top chord of the substitute Vierendeel model.

4.2 Maximum edge stresses as a result of the introduction of vertical traffic loads

Moving a unity concentrated vertical load horizontally along the top edge of the web post renders an influence line for the stress at the critical point on the edge of the web cutout due to vertical load introduction (Fig. 5). For the cutout type as proposed by Haibach, this critical location is found at the point of minimal post width. For other cutout geometries this point may be at a different location, either closer to or further away from the lowest point of the connection of the web with the rib. For the numerical example (Table 1), the influence line and the critical location are given in Fig. 5. Since the influence line can only be computed for vertical roads on the web area between the ribs, it requires extension beyond this limited scope. The methods applies linear extension to zero at points A and B (Fig. 5). Loads beyond these points are not to be considered.

4.3 Maximum edge stresses as a result of the Vierendeel action

For this purpose a uniformly distributed horizontal unity line load is applied at the top edge of the web post. Firstly the horizontal deformation, taken at the midpoint of the top edge (Fig. 6), is stored. As already pointed out, this deformation can be linked to an equivalent stiffness parameter. Subsequently, the maximum edge stresses at the two critical points located on the edges of the web cutout are stored (Fig. 7). Due to symmetry, both values are equal in amplitude and of opposite sign. Evidently, in all cases the values to be considered are the principal stresses, parallel to the cutout edge. However, in the particular case of the Haibach cutout shape, the maximum principal stress at the critical location has vertical orientation.

Finally, since the maximum stresses are found due to a unity horizontal load, they form a link between the horizontal shear forces from the Vierendeel model and the actual stresses at the cutout edge. Moreover, they depend on the cutout geometry only and may be called “shape factor”.

Fig. 8 depicts vertical stresses due to a unity horizontal load at the top edge in a horizontal cut (Fig. 7)

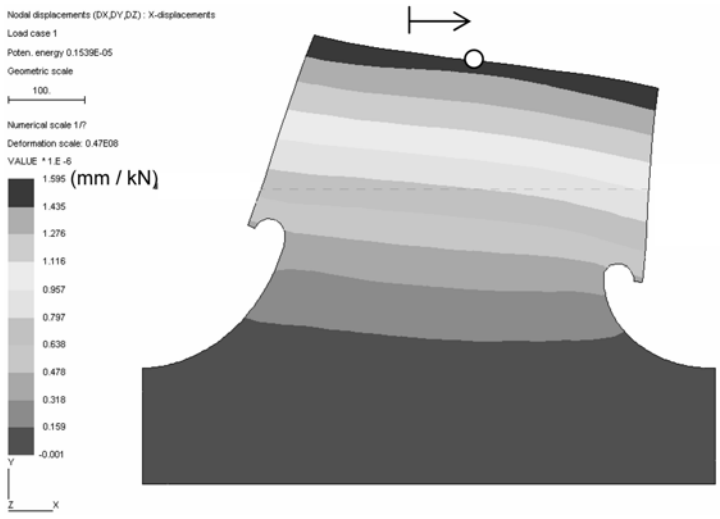

Fig. 6 Horizontal displacements of the single tooth model caused by a horizontal unity load on the top edge

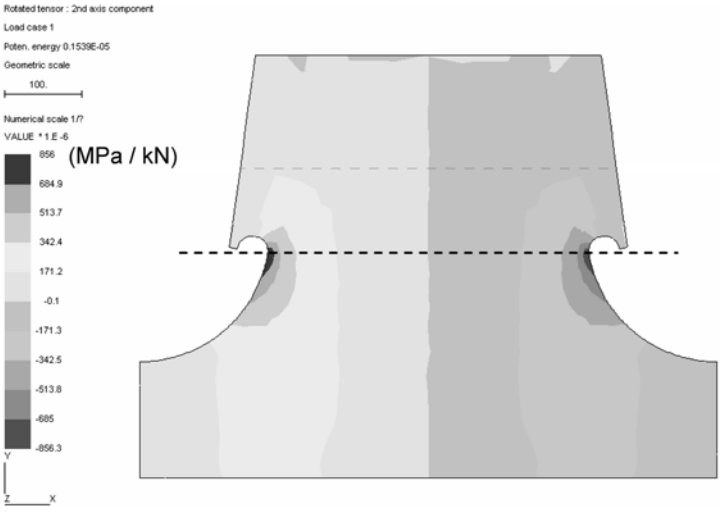

Fig. 7 Vertical stresses caused by a horizontal unity load on the top edge

containing the critical locations of the Haibach cutout. Clearly, when a horizontal transverse cut is made, the resulting stress pattern certainly does not correspond to a triangular distribution, proving the need for the proposed adaptation to the Haibach method. This figure also shows the triangular stresses as they would have been computed by the original Haibach method. The stress concentration factor approaches 2 consistently. It may be noticed that for this cutout type the critical locations for introduction of vertical traffic loads and for Vierendeel action coincide. This is not the case for many other cutout shapes.

4.4 Assessment of the flexural stiffness of the vertical posts

Although in the Vierendeel analogy they are treated as such, the vertical posts clearly do not comply

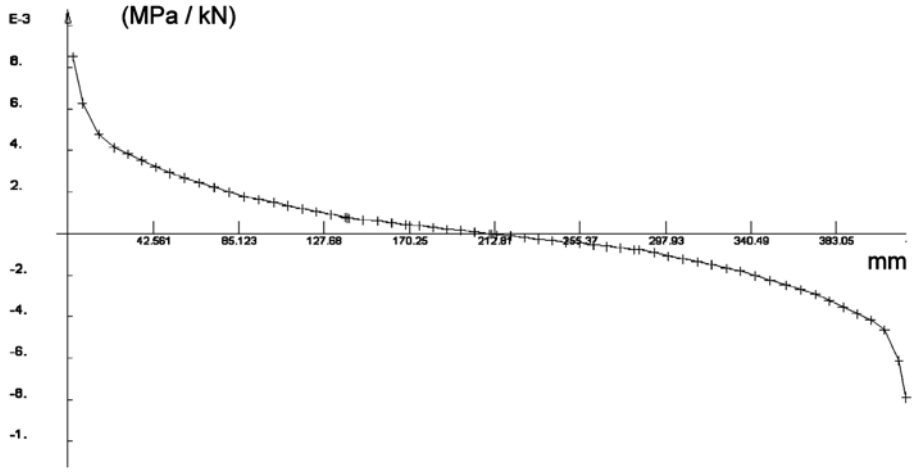

Fig. 8 Distribution of vertical stresses along the horizontal cut in Fig. 7

with the assumptions of simple bending beam theory, since the height to span ratio is too large. In such a case, shear deformation needs to be taken into account. In the analogy, a vertical post is assumed to be rigidly connected to the lower chord and pinned to the upper chord. Without considering shear deformation, the relation between load and horizontal deformation would be given by the simple expression Eq. (1) for cantilever beams:

$$u_p = \frac{P \cdot h_p^3}{3EI_p} \tag{1}$$

If on the other hand both flexural as well as shear deformation are considered, the relation is given by expression Eq. (2):

$$u_p = \frac{P \cdot h_p^3}{3EI_p} + \frac{3}{2}\frac{P \cdot h_p}{GA_p} \tag{2}$$

Depending on the post geometry, expression Eq. (1) will underestimate the actual horizontal deformation of the post many times. Consequently, any internal force and moment distribution calculated with the Vierendeel model without considering shear deformation in the vertical posts will be incorrect since the shear connection between upper and lower flange provided by the vertical posts is much weaker than is assumed by expression Eq. (1).

Standard available framework analysis software generally does not account for shear deformation. In view of this, a possible procedure consists of introducing an equivalent flexural stiffness corresponding to equal deformation at the top chord. This equivalency is expressed by Eq. (3):

$$\frac{P \cdot h_p^3}{3EI_{equiv}} = u = \frac{P \cdot h_p^3}{3EI_p} + \frac{3}{2}\frac{P \cdot h_p}{GA_p} \tag{3}$$

This relation can be transformed into a practical formula Eq. (4) for the calculation of an equivalent flexural stiffness (See Fig. 9):

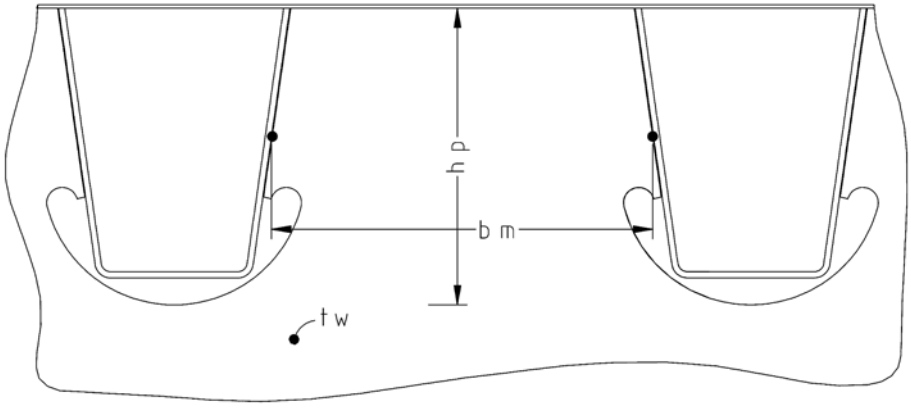

Fig. 9 Dimensional notations of the floorbeam

Table 2 Equivalent flexural stiffness parameter as calculated by different methods

I (no shear)	$214{,}64.10^6$ mm^4
I_{equiv} (Eq. 4)	$84{,}04.10^6$ mm^4
I_{equiv} (Eq. 5)	$67{,}80.10^6$ mm^4

$$I_{equiv} = \frac{t_w \cdot b_m^3 \cdot h_p^2}{12 \cdot h_p^2 + 9 \cdot b_m^2 \cdot (1 + \upsilon)} \tag{4}$$

After replacing the posts stiffness by expression Eq. (4), standard framework analysis software can be used in a straightforward manner.

Another possibility is the explicit use of the deformations from the horizontal unity load case as stored from the 2D finite element model. Then, the equivalent flexural stiffness may be taken from Eq. (5):

$$I_{equiv} = \frac{P \cdot l^3}{3E \cdot u_{F.E.M.}} \tag{5}$$

where: $u_{F.E.M.}$ = horizontal deflection at the top of the F.E. model (Fig. 6) for a horizontal load P.

With the characteristics of the numerical example the values of I_{equiv} of Table 2 are found. The values computed from expressions Eq. (4) and Eq. (5) differ by 25%, a relatively small amount compared to the 300% difference if no shear deformation is considered. Evidently, the difference between the pure flexural stiffness and the equivalent flexural stiffness value increases with larger rib spacing and smaller rib heights. For realistic rib dimensions and spacing the adaptation certainly becomes necessary.

4.5 Introduction of vertical stresses calculated by full finite element modelling

Stresses in the vertical post model due to introduction of vertical traffic loads can be easily compared to the values found from the fully supported finite element floorbeam model (Fig. 10) by applying concentrated patch loads on the deckplate directly above the web along the length of the floorbeam. As verified easily, the results are independent from which web area between two adjacent ribs is under

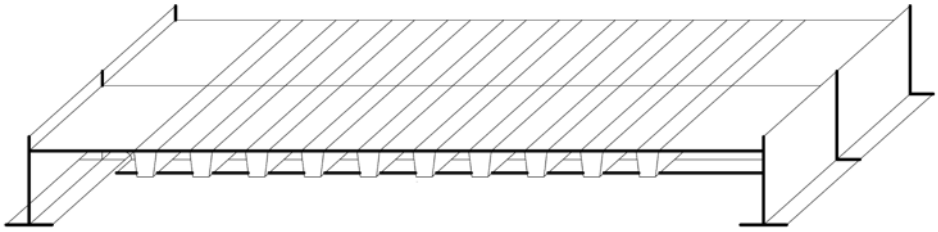

Fig. 10 Finite element model for the complete floorbeam including longitudinal ribs

consideration. By introduction of concentrated unity patch loads on the deck plate, a similar influence line for local load introduction can be created (Fig. 11). This influence line can be compared to the one depicted in Fig. 5. Although the vertical post model is relatively crude concerning its boundary conditions, both influence lines of Fig. 11 practically coincide, proving the applicability of the 2D model.

4.6 Truss action stresses calculated by full finite element modelling

Identical patch loads can also by applied to the beam as it is actually integrated in the whole structure. The edge stresses in each of the critical points appearing to the left and to the right of each rib make up a series of influence lines. Clearly these stresses are a combination of a Vierendeel component and a vertical load introduction component. Since the aim is to focus on the Vierendeel action, the components created by local introduction as stored previously need to be subtracted from the combined results.

For the numerical example the influence lines are given in Fig. 12. It should be pointed out that in Fig. 12 for clarity reasons, the sign of the values left of each stiffener has been switched. If the Vierendeel analogy is correct, a stress value found left of a rib would have to be equal to the absolute value right of the rib but with opposite sign, since in the Vierendeel analogy both points correspond to a single vertical post. As in Fig. 12 all left hand side values have reversed sign, they should be equal to or at least close to the right hand side values from the previous stiffener (e.g. 2Left = 1Right; 3Left = 2Right, etc.). Clearly this is the case, and the applicability of the Vierendeel method is hereby proven.

The influence lines can now be compared to the results found from the Vierendeel framework

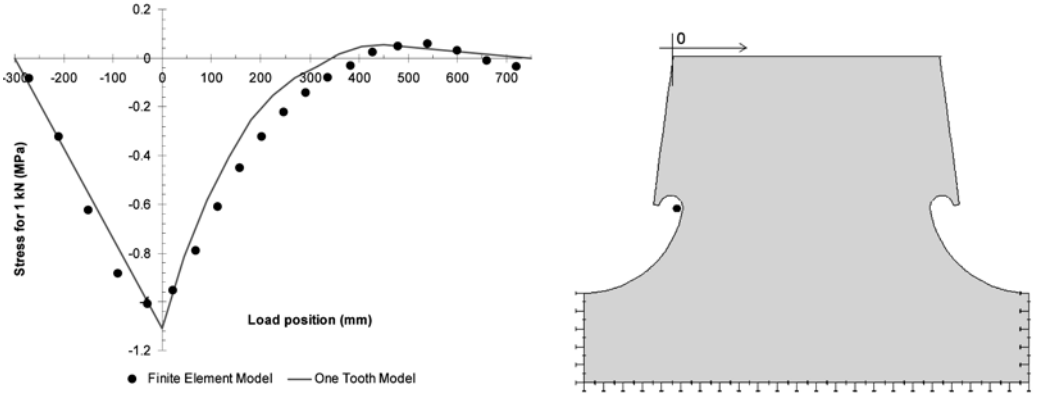

Fig. 11 Comparison of results for the introduction of vertical traffic loads

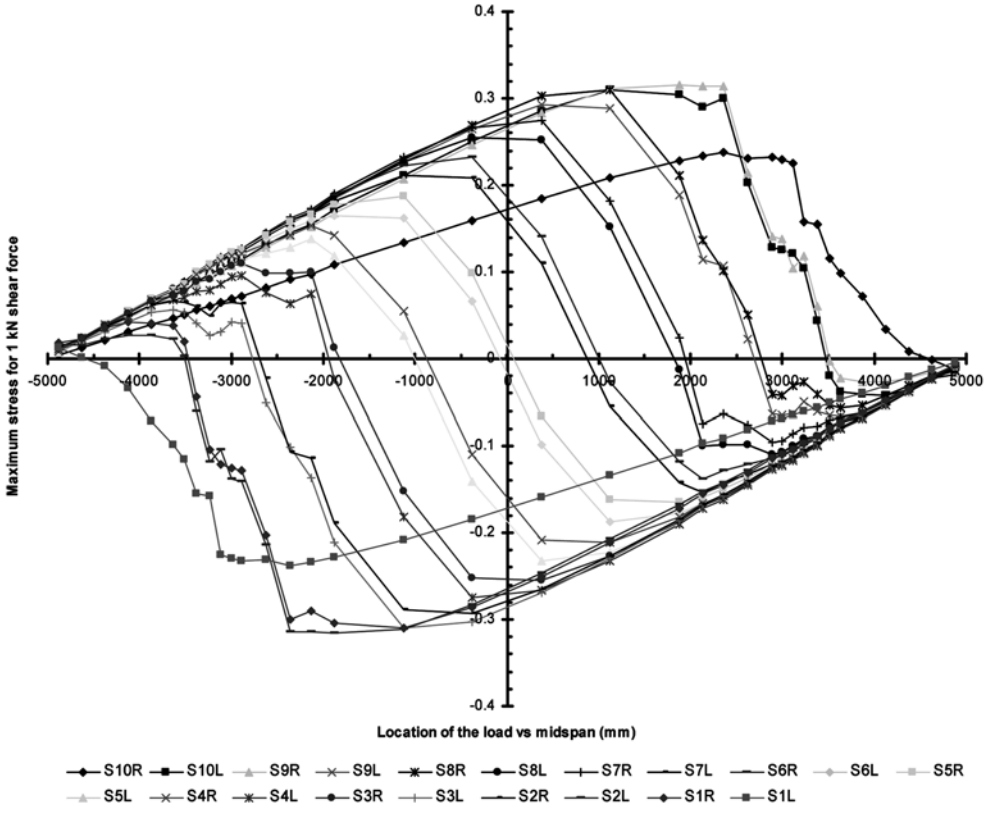

Fig. 12 Stresses caused by Vierendeel action in the critical points of the various vertical posts

Fig. 13 The Vierendeel model used to illustrate the truss action

analysis multiplied by the shape factor. Fig. 13 illustrates the Vierendeel model used for this purpose. In a similar way as was done in the full FE model and by applying unit loads on the top chord of the girder, similar influence lines can be generated for the horizontal shear forces in each of the vertical posts. Since they result from a framework analysis the results are not influenced by local load introduction. Fig. 14 visualises these influence lines for the numerical example. The influence values from Fig. 14 multiplied by the shape factor should equal the influence lines from Fig. 12. Qualitative correspondence with Fig. 12 is evident, and in order to verify whether the combination method provides a quantitative match as well the explicit stress comparison for the posts 2 to 6 are given in Fig. 15. Due to symmetry, post 7 to 10 need no consideration. For each of the posts being considered an excellent correspondence is found. This proves the validity of the combination model for the numerical example. Noticeably, comparison for the first and last vertical post is impossible, since for these posts the shape factor cannot be calculated.

Other combinations of realistic dimensions can be now examined, since the combination model for the dimensions of the numerical example has been validated.

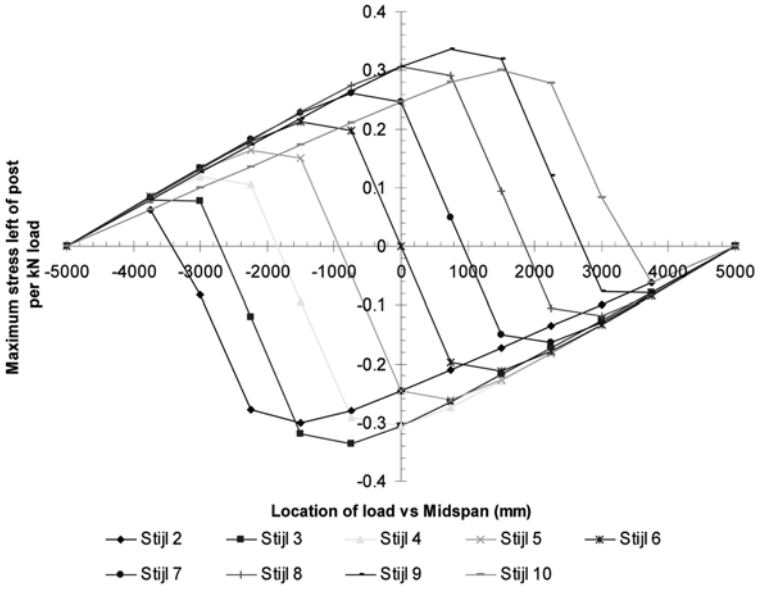

Fig. 14 Influence lines for the horizontal shear forces in the vertical posts (Vierendeel model)

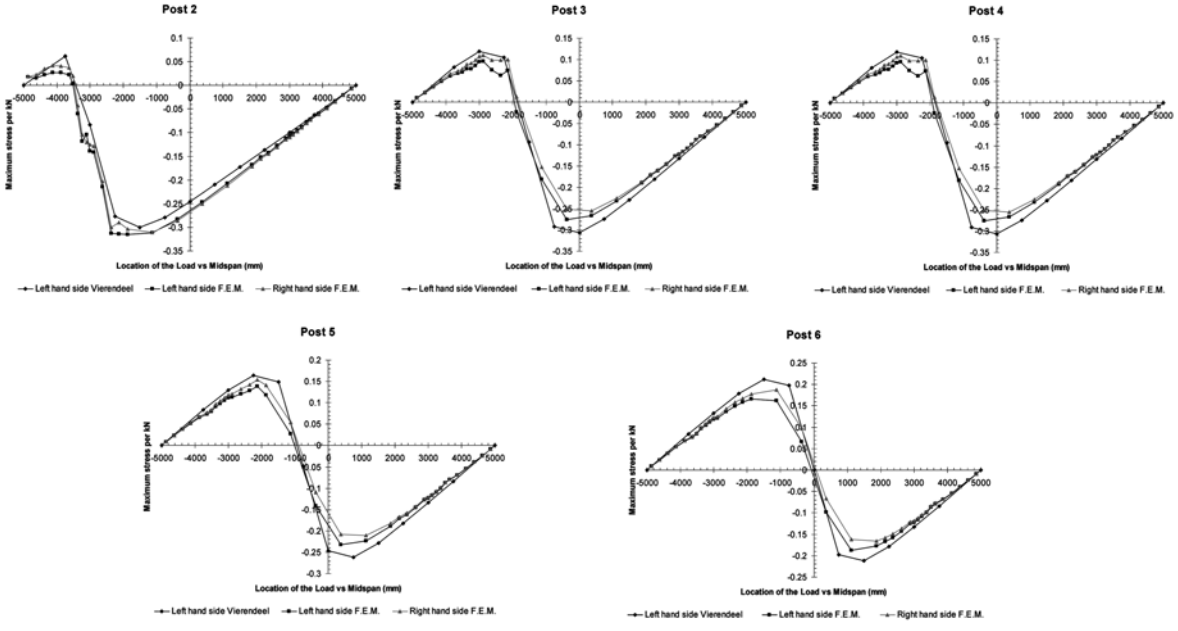

Fig. 15 Comparison of results from the combination model to full finite element results

5. The validity of the combination model – a limited parametric study

The combination model can be validated further for other dimensions by comparing the results in the web area between the first and second rib, equal to the second vertical post in the combination model, and this for a load acting above the 4th post. This load position generates the largest truss related

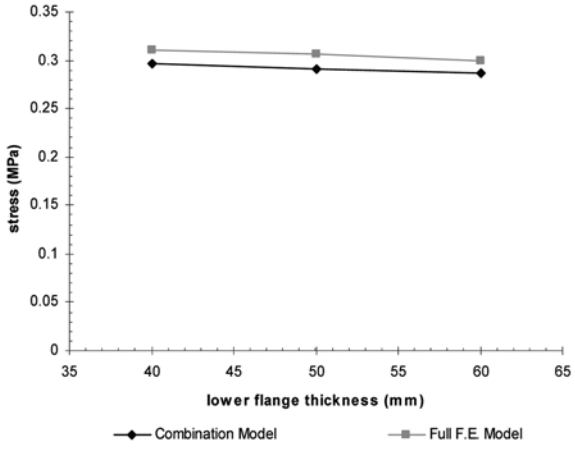

Fig. 16 Calculated stresses for different lower flange thicknesses

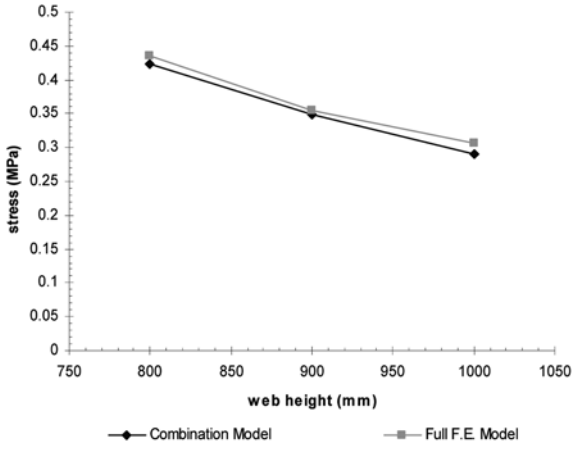

Fig. 17 Calculated stresses for different web heights

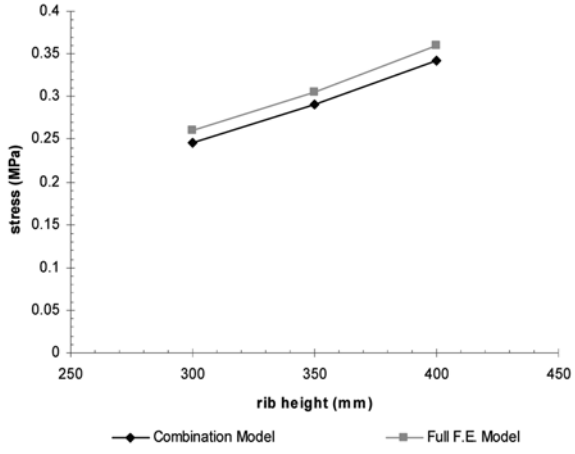

Fig. 18 Calculated stresses for different rib heights

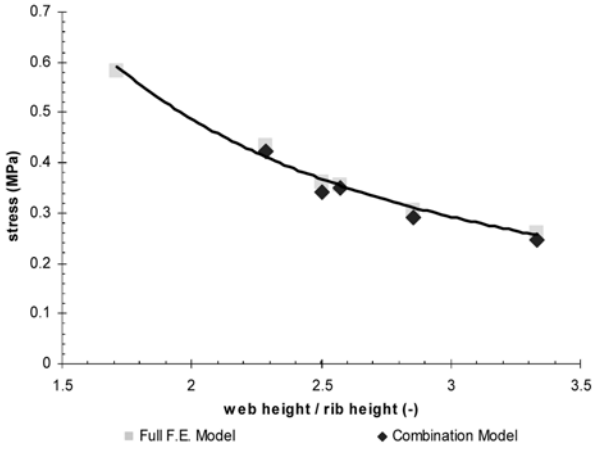

Fig. 19 Calculated stresses for different web height to rib height ratios

stresses, occurring in the second vertical post. Figs. 16 to 18 give comparative results of maximum truss related stress in the web area between the first and second rib for a unit load acting above the 4th post, while varying the thickness of the lower flange of the floorbeam, the floorbeam height and the rib height.

For these 3 series of dimensional variations, the combination model follows the changes in maximum stresses correctly. The error margin between full FE and combination model results remains small. The combination model thus appears to be applicable for a wide range of floorbeam topologies.

Concerning the recommendations for floorbeam web height to stiffener web height restrictions, an important conclusion emerges. Fig. 19 gives stress results at the critical location as a function of the floorweb height to rib height ratio. According to European researchers (Bruls 1995), the ratio gives a boundary for the use of rib to floorbeam intersections with of without additional web cutout. For ratios higher than or equal to 3, an additional cutout may be used, but for lower ratios the connection should be welded all round. Obviously, the graph of Fig. 19 is only slightly non linear, and cannot be the base

of a boundary. This indicates that the limitation of the floorbeam to rib height ratio might not be the principal governing factor in the choice of the rib to floorbeam joint.

An important point of notice is the influence of the minimum element size on the shape factor in a finite element calculation. When comparing results of the combination model to results of the full finite element model, the grid dimensions should be of equal size in both cases. Reducing grid size will inevitably raise the magnitude of the shape factor. This observation is very important for all design issues concerning maximum stresses at the cutout edge. Even when comparing calculated values to measured values (De Corte and Van Bogaert 2002, 2004, De Corte 2004, De Corte *et al.* 2004(a), 2004(b)), one should bear in mind that strain gauges have finite dimensions. The measured strain will be a mean value across the active grid. This corresponds to deriving a mean value across one or more finite elements. For example, if an active gridlength of 5 mm is used, it is useless to compare the measured result to the maximum value found from a finite element analysis with 1 mm element dimension length. In such case, an average value over all elements corresponding to the active grid should be considered.

6. Alternative web cutout shapes

6.1 General comparison

The combination model enables comparing different alternative additional cutout geometries without having to know the full floorbeam geometry. Fig. 20 gives ten alternatives, considered in De Corte (2005). The basic model has a rib spacing of 600 mm and a rib height of 300 mm. The ribs are closed trapezoidal ribs (upper width = 300 mm / lower width = 200 mm). For the basic geometry as proposed by Haibach, the locations of maximum stress due to Vierendeel action and local load introduction coincide. For other geometries both locations may be different.

An analysis of shape factors and maxima of load introduction influence lines demonstrates

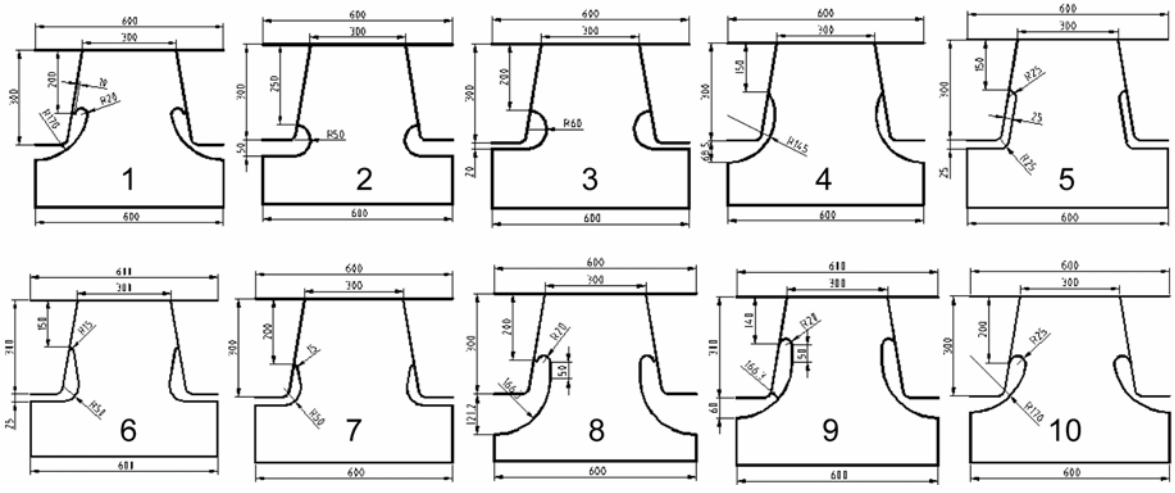

Fig. 20 Alternative cutout geometries

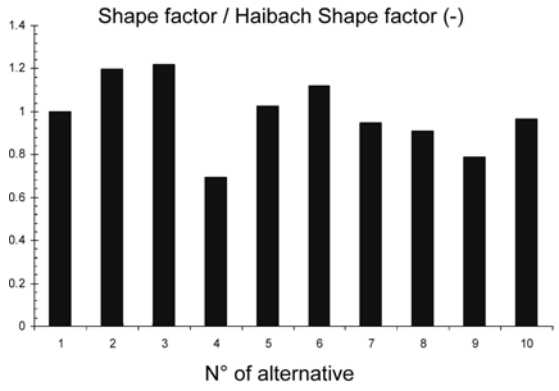

Fig. 21 Shape factor relative to Haibach shape factor for different cutout alternatives

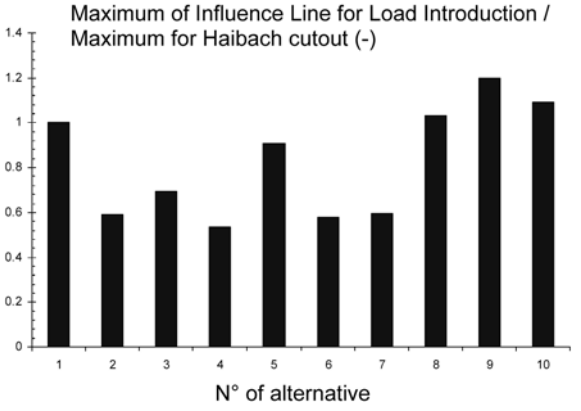

Fig. 22 Load introduction maximum relative to Haibach maximum for different cutout alternatives

substantial differences for the various cutout shapes. A first comparison is given Fig. 21 showing values of the ratio of the shape factor to the factor corresponding to the Haibach geometry. This figure indicates that shape factor values can be up to 25% higher and 35% lower, compared to the Haibach shape. The best performing shape clearly is the circular cutout. A second comparison is given in Fig. 22 showing values of the maxima of the influence line for vertical concentrated load introduction. Clearly the Haibach shape and similar shapes are less useful for high local load introduction, since a reduction of nearly 40% is achieved for a number of alternatives. Haibach shaped cutouts are more useful for situations with wide spread loads such as in railways rather than concentrated highway loads. Indeed the Haibach shape was first intended for railway bridges.

The circular shaped opening appears to be advantageous, as conformed by Lehrke (1989). However, should there be negative effects from stiffener distortion, the web opening created by circular cutouts is too large, the stiffener to floorbeam joint length becoming too small (Bruls 1995). Because of this, the use of large circular cutouts is not recommended. Overall, alternative number 7 is advantageous for Vierendeel girder action as well as for local load introduction. This result is confirmed by full F.E. analysis.

6.2 Alternative 7

The shape of alternative 7 features a horizontal lower edge and a slope parallel to the opposite rib wall connected by an arc with a 50 mm radius. Each rib wall is welded to the floorbeam web along two thirds of its height, thus minimising rib distortion problems. This is in contrast to the circular opening of alternative 4, where welding is done over only 50% of the rib height. For alternative 7, the critical points for Vierendeel action and for vertical load introduction do not coincide. Both points are marked in Fig. 23 by a filled (local vertical load introduction) and a blank dot (Vierendeel truss action). Therefore, the load introduction related stresses are reduced significantly at the point of maximum Vierendeel related stresses and vice versa. Clearly, direct addition of two maximum values is no longer the most governing situation, favorising further the alternative 7 over the Haibach cutout shape. Summarising this, the use of alternative 7 would imply a 10% reduction of Vierendeel stresses, a 40% decrease of vertical load introduction stresses, and the non-coincidence of both. Evidently, this alternative is worth further investigation.

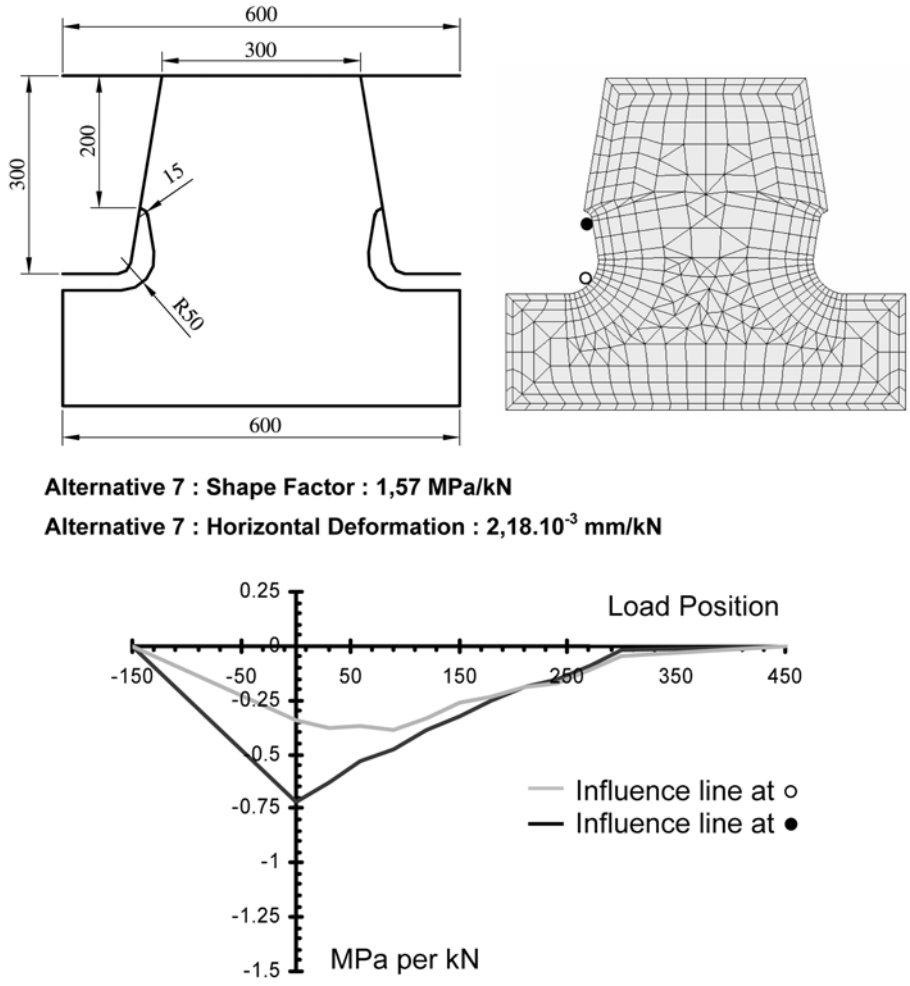

Fig. 23 Details of results for alternative 7

7. Conclusions

A floorbeam of an orthotropic plated bridge deck is subjected to a combination of Vierendeel action and the local introduction of vertical traffic loads. In this paper a combination model is presented for the stepwise calculation of the stresses at the edges of the web cutouts. In a first step a detailed single post finite element model with the exact cutout shape is created. With this model an influence line for vertical loads is assembled. Additionally, the horizontal displacements and the maximum principal stresses for horizontal loads applied at the top edge are stored for further use. In a second step a substitute Vierendeel framework model of the floorbeam is analysed. The combination of both steps eventually leads to the location of the fatigue - critical points as well as the corresponding stress values. The principle is illustrated by a numerical example and is verified for various dimensions.

With this method, alternatives for additional cutout geometries can be compared more rationally. There is no need to implicate the other floorbeam characteristics in the comparison. Finally, the results

of a study of various alternatives shows that optimisation is possible, although other effects such as stiffener distortion might also need attention. Further research is certainly required for field verification of the proposed cutout geometry as well as for assessment of the influence of stiffener distortion and of out of plane web deformations.

References

Beales, C. (1990), "Assessment of trough to crossbeam connections in orthotropic steel bridge decks", TRRL Research Report 276, Crowthorne, UK.

Bruls, A. (1995), "Common synthesis report : measurements and interpretation of dynamic loads on bridges, Phase 4 : fatigue strength of steel bridges", ECSC, Brussels, Belgium.

De Corte, W. and Van Bogaert, Ph. (2000), "Assessment of cross beam fatigue in orthotropic plated bridge decks by measurement-complying influence lines", *Proc. of the Int. Conf. on Steel Structures of the 2000's*, Istanbul, Turkey, September.

De Corte, W. and Van Bogaert, Ph. (2002), "Fatigue assessment of orthotropic bridge crossbeams : a combined framework – F.E. approach", *Eurosteel 2002,* Coimbra, Portugal, September.

De Corte, W., Van Bogaert, Ph., De Backer, H. and De Pauw, B. (2004), "Orthotropic plated bridge deck analysis : A road railway comparison", *Proc. of the 10th Nordic Steel Conference*, Copenhagen, Denmark, June.

De Corte, W. (2004), "Assessment of fatigue strength of steel orthotropic plated bridge decks from continuous measured stress spectra", *Proc. of the 1st Orthotropic Bridge Conference*, Sacramento, CA, United States, August.

De Corte, W. and Van Bogaert, Ph. (2004), "Fatigue strength verification of a steel orthotropic plated bridge deck for railway traffic", *Proc. of the 1st Orthotropic Bridge Conference*, Sacramento CA, United States, August.

De Corte, W., Van Bogaert, Ph., De Backer, H. and De Pauw, B. (2004), "Verification of local and global action of a tied arch railway bridge with orthotropic deck during consecutive test phases", *Arch '04*, Barcelona, Spain, November.

De Corte, W. (2005), "Fatigue of steel orthotropic plated bridge decks subject to traffic loads", Ph Thesis, Academia Press, Ghent, 2005 (in Dutch).

De Corte, W. and Van Bogaert, Ph. (2006), "The effect on the moment distribution in orthotropic plated decks of shear deformation in floor beams : an addition to the Pelikan – Esslinger method", *J. Constr. Steel Res.*, to be published.

Dexter, R. and Fisher, J. (1995), "Fatigue cracking of orthotropic steel decks", *Proc. of the Nordic Steel Conference 1995*, Malmö, Sweden.

Haibach, E. and Pläsil, I. (1983), "Untersuchungen zur Betriebsfestigkeit von Stahlleichtfahrbahnen mit Trapezhohlsteifen im Eisenbahnbrückenbau", *Der Stahlbau*, 9/**83**, 269-274.

Lehrke, H. (1989), *Messung und Interpretation von dynamischen Lasten an Stahlbrücken. Phase 3 : Schwingungsfestigkeitsverhalten von orthotropen Platten in Stahlstraßenbrücken*, Fraunhofer-Institut für Betriebsfestigkeit, Darmstadt, Germany.

Pelikan, W. and Esslinger, M. (1957), *Die Stahlfahrbahn – Berechnung und Konstruktion*, M.A.N. Forschungsheft, N°7.

Troitsky, M.S. (1968), *Orthotropic Bridges: Theory and Design,* 2nd Printing, Cleveland, Ohio.

Van Bogaert, Ph. and De Corte, W. (2001), "Influence of crossbeam topology on the stress distribution in closed stiffener orthotropic bridge decks", *Proc. of the First Int. Conf on Steel & Composite Structures*, Pusan, Korea.

Wolchuk, R. (1963), *Design Manual for Orthotropic Steel Plate Deck Bridges*, AISC.

Wolchuk, R. (1992), "Secondary stresses in closed orthotropic deck ribs at floor beams", *J. Struct. Eng.*, **118**(2), 582-595.

DN